Numerical Modeling and Seismic Assessment of Columns Reinforced by Smooth Rebars

**M. Arabpanahan, M. S. Marefat, M. Khanmohammadi &
E. Norouzzadeh Tochaei**
College of Engineering, School of Civil Engineering, University of Tehran, Tehran, Iran

15 WCEE
LISBOA 2012

SUMMARY:
There are many concrete structures that have been constructed before 1970, and have been reinforced by plain bars. For retrofitting these structures, it is necessary to investigate seismic performance of them, and to evaluate their ductility, strength, stiffness and energy dissipation. The objective of the present paper is to propose a numerical model to simulate the response of concrete columns with old design details, i.e., reinforced by smooth bars. The model is based on bond-slip properties of smooth bars derived from pullout tests. The global behavior, then, is calibrated by results of cyclic and monotonic tests performed on four concrete columns reinforced by smooth bars. The numerical modeling carried out by MATLAB programming, considers three displacement components of column, under lateral and axial loads simultaneously; flexure, slip, and shear. Also in this model, the rocking mode as a result of slip contribution is investigated.

Keywords: Reinforced concrete, Smooth (plain) bar, Seismic assessment

1. INTRODUCTION

Seismic behavior of reinforced concrete structures with smooth bars is an important case of question for engineers and researchers. This issue becomes more significant for seismic assessment and rehabilitation of these structures. This significance is because of obvious performance differences between concrete structures reinforced by smooth bars and those reinforced by deformed bars. That is because of bond inherence between smooth bar and concrete that surrounds it. In other words, slippage of smooth bar in concrete due to bond strength deterioration, creates special behavior for this kind of structures. In this paper, reinforced concrete columns with smooth bars, are modeled and investigated. Experimental modeling on this members by Verderame et al. (2008a and 2008b), Arani et al. (2010) and Yalcin et al. (2006) showed that under lateral and axial load to a simple curvature column, the majority portion of the deflection, on the index point (at the level of exerting lateral load), is related to "fixed end rotation". In other words, they observed that the crack opening at the interface of column and footing is the most important cause of deflection in the index point of column, especially in upper drifts. To achieve slip because of bond deterioration, variety ranges of models have been presented. Feldman and Bartlett (2007) and Verderame et al. (2009(b)), by experimenting on pullout specimens, introduced bond- slip models (Fig. 1.1). By using each of these models the resistant bond force that acts against pullout tension load in companion of restraint force created from hook or each mechanical implementation at the end of the bar (in column or in the footing) can be achieved. Behavioural hook model presented by Fabbrocino et al (2005), indicates a nonlinear relationship, between hook slip and stress, at the beginning point of the hook.

The base crack that is one of two or three main ones formed on the columns reinforced with smooth bars, can be known as a result of tension bar slippage either in footing or in the column element. As Arani et al. (2010) claimed this phenomena can entail a behavioural mode called rocking mode (especially in specimen under cyclic loads). By that description, rotational capacity of these members, is higher than similar ones with deformed bars. Modelling of rocking elements by Roh and Reinhorn

(2009), showed that after passing cracking and yield states, these elements reach to beginning of rocking phase (at the maximum lateral strength).
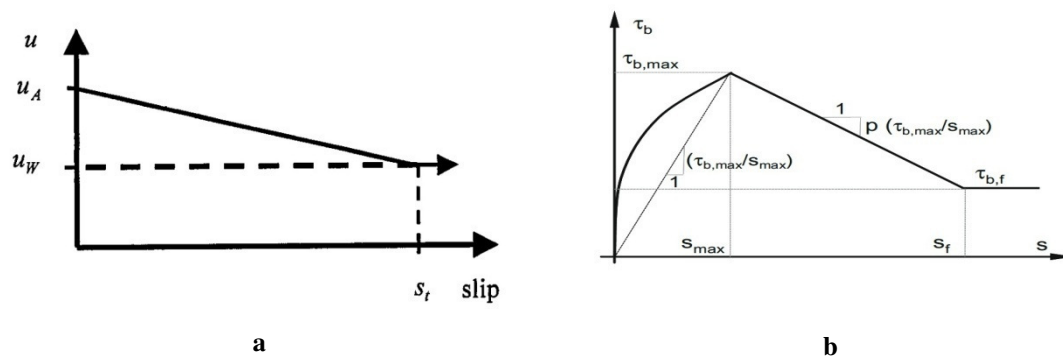
Figure 1.1. Bond-slip proposed models represented by: a) Feldman et al. (2007) and b) Verderame et al. (2009b)

In concrete columns reinforced by smooth bars, because of obvious column uplifting from the base, rocking mode is formed, but because of residual bond resistance between tension bar and concrete, and also yield strength of bar, this column uplift is limited and rocking mode is controlled. Predominant mode (rocking) is influenced by both lateral displacement and lateral strength of column. Arabpanahan et al. (2012), achieved to the lateral displacement by taking account slip of bar both in column element and footing. In the present paper the lateral strength of column as a function of P-Δ concept is investigated. Indeed the objective of this paper is to develop the model presented by latter authors. Eventually by performing a statistical analysis on outputs of numerical model, behavioral components of these members are assessed.

2. MODELLING OF ROCKING MODE

Rigid body rotation of RC columns with smooth bars entails rocking action. The influence of restricted rocking mode on behavioral curve of column element will be explained.

2.1. The Influence on Strength

This impact is investigated by considering P-Δ role on lateral strength. Despite in RC columns with deformed bars, P-Δ increases moment demand at the base, in those reinforced by smooth bars, because of column uplifting from the base, the behavior is different. In other words in a RC column reinforced by deformed bars, that flexure is the dominant mode, the impact point of axial reaction force is approximately constant and coincident to intersection of column center line and foundation surface (by assuming that there is no obvious column uplifting from the base). Fig. 2.1 shows typical columns reinforced by deformed and smooth bars under both axial and lateral loads.

So as is showed in (a) by having a constant impact point of axial load reaction and increasing the lateral displacement of index point, the demand moment at the base is added. But in those reinforced by smooth bars, because of change in contact depth of column and footing and resulting continuous changes in impact point of axial reaction load, the influence of P-Δ is quite different. As is recognizable in P-Δ term, $\Delta=\Delta_0$ and that is the horizontal distance between exerting axial load point and reaction impact point of axial load, so Δ_0 doesn't have a unique basis. In following steps the impact of P-Δ will be summarized.

1) The axial load exerting point is further than the axial load reaction impact point and the majority depth of critical section is under compression. This behavior is similar to conventional columns reinforced by smooth bars and P-Δ entails in base moment demand increasing.
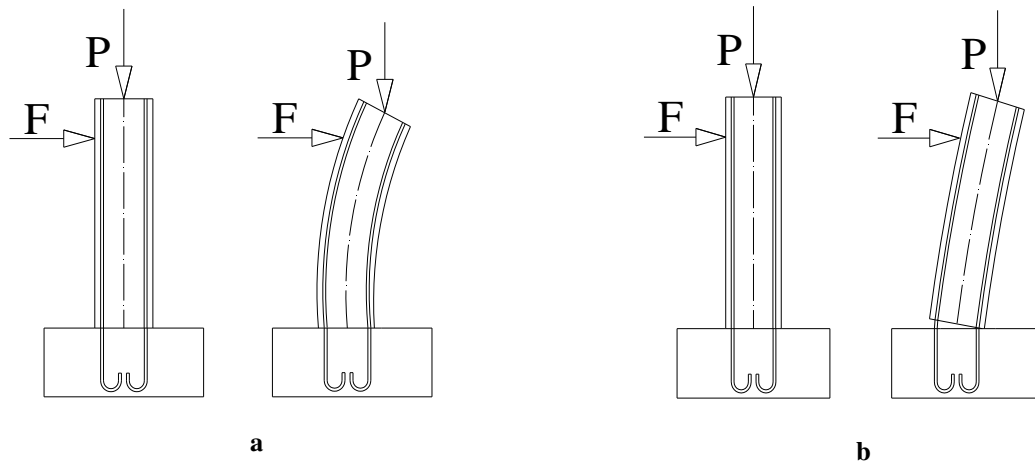
Figure 2.1. Deformed shaped of reinforced concrete column: a. By Deformed bars b. By Smooth bars

2) The axial load reaction impact point, further than the axial load exerting point, so in this step, P-Δ decreases demand moment at the base and increase lateral strength of column, because the moment resulting from P-Δ, works in opposite direction of demand moment of lateral load.
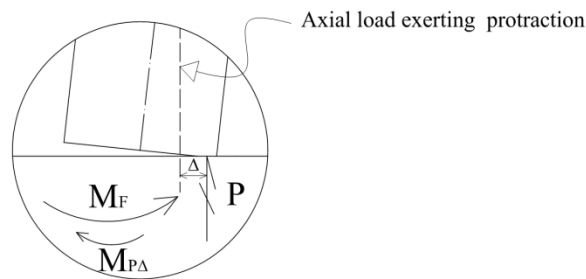
Figure 2.2. Reaction moments caused at the column base

Above illustration can be seen in the next relationship:

$$M_{base} = M_F - M_{P\Delta} = F.L - P.\Delta \qquad (2.1)$$

3) And finally, the axial load exerting point, go further again in comparison with axial load reaction impact point, and axial load higher the demand moment at the base (column's critical section).

2.1.1. Geometrical Solution

For rocking elements that have significant end rotation, it is necessary to solve the real geometrical deflection at index point of column. To achieve this objective, it is assumed that the top of column (inflection point), goes on a circular path during the loading process. Fig. 2.3 shows the deformed shape of RC column with smooth bars that rocking action dominates its behavior.

In Fig. 2.3, L and L_{shear} are total height and shear height (shear span) of column respectively, $L^{'}$ and $L^{'}_{shear}$ are deformed height and deformed shear height of column due to loads respectively, Δ is displacement at the index point and finally, θ and γ are axial load rotation and lateral load rotation, respectively. The latter parameters are achieved by a simple geometric solution as is described after Fig. 2.3.
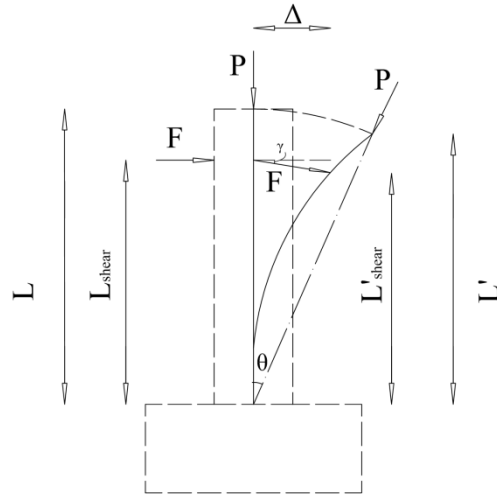
Figure 2.3. Deformed shape of rocking column and changes in loading direction

$$\gamma = \tan^{-1}\left(\frac{L_{shear} - L'_{shear}}{\Delta}\right) \tag{2.2}$$

$$\theta_{elastic} = \int_0^L \frac{\varphi(x)}{L}dx + \frac{S}{d-c} \tag{2.3}$$

$$\theta_{plastic} = \int_0^L \frac{\varphi_y x}{L}dx + \left(\varphi(x) - \varphi_y L_P\right) + \frac{S}{d-c} \tag{2.4}$$

where $\theta_{elastic}$ and $\theta_{plastic}$ are the base rotations before and after yield of section respectively, $\phi(x)$ and ϕ_y are curvature distribution along the length and yield curvature of critical section (in 1/mm), respectively, S is total slippage of extreme tension bar in section accumulated at the interface of column element and footing (in mm), d is effective depth of section (in mm), c is compression depth of section (neutral axis height) (in mm) and L_p is the plastic hinge length (in mm) calculated from the relationship proposed by Paulay and Priestley (1992):

$$L_p = 0.08L_{shear} + 0.022f_y D_b \tag{2.5}$$

where D_b is the diameter of largest bar in the section (in mm) and f_y is the yield strength of bar (in MPa). Other variables were defined before and go to the relationship (in mm).

Demand moment (M_{base}) and base shear (V_{base}) resulting from horizontal and vertical components, of lateral and axial inclined loads, can be calculated from the next relationships:

$$M_{base} = F\left[L'_{shear}\cos\gamma + (\Delta + 0.5c - H)\sin\gamma\right] + P\left[\left(\Delta_{top} - 0.5H + 0.5c\right)\cos\theta - L'\sin\theta\right] \tag{2.6}$$

$$V_{base} = F\cos\gamma - P\sin\theta \tag{2.7}$$

where H is the column section height in mm and Δ_{top} is the lateral displacement at the top of the column (not the index point). Other parameters were defined before. It is remarked that by using above relationships, the triple behavioral steps originated from P-Δ concept in rocking element, that were introduced before, are considered automatically.

For rocking elements in this paper it is assumed that the impact point of axial load reaction is coincident with the center of compression depth in contact surface and the column rotates around the neutral axis.

2.2. The Influence on Displacement

To achieve the behavioral curve, that is needed to determine displacement corresponding to the base shear. Components of displacement in a RC column with smooth bars come below:

$$\Delta_{total} = \Delta_{flexure} + \Delta_{slip} + \Delta_{shear} \tag{2.8}$$

Calculating of $\Delta_{flexure}$ is similar to calculation of that for conventional columns reinforced by deformed bars. Having strain distribution curvature of each section along the column length and by curvature integrating twice along the shear length, flexural deformation at the index point can be achieved. In order to verify the flexural performance of the rocking model, M- ϕ curves of model are compared with outputs of KSU- RC software (released by Kansas State University). (Fig. 2.4)

Shear displacement (Δ_{shear}) is averagely 5% of summation of slip and flexure displacements (Arani et al. 2010). So in the numerical modeling, based on experimental results it is assumed that it has a low contribution to the total displacement.

Slippage displacement (Δ_{slip}) is because of deep crack opening at the interface of column and footing as a result of bar slip in both footing and column element. So linear model proposed by Feldman and Barttlet (2007) to represent the bond behavior of concrete and smooth bar is used:

$$u_A / \sqrt{f_c^{'}} = (0.19 - 0.07k_{sz} + 0.05k_{sh})\sqrt{R_y} + (-2.7 \times 10^{-5} + 4.0 \times 10^{-5}k_{sz} - 3.0 \times 10^{-5}k_{sh})L_dR_y \tag{2.9}$$

$$u_W / \sqrt{f_c^{'}} = (0.042 - 0.01k_{sz} - 0.003k_{sh})\sqrt{R_y} + (-1.64 \times 10^{-5} + 4.28 \times 10^{-6}k_{sh})L_dR_y \tag{2.10}$$

where $u_A / \sqrt{f_c^{'}}$ and $u_W / \sqrt{f_c^{'}}$ are expressed in $\sqrt{MPa}$, k_{sz} is an indicator variable for bar size equal to zero for less than 16 mm bars and 1 for more than 32mm bars, k_{sh} is an indicator variable for bar shape equal to zero for round bars and 1 for square bars, R_y is bar surface roughness (in μm) and L_d is development length of the bar in concrete. R_y has been measured by Feldman for ordinary smooth bars and was determined to be equal to 3.1 μm.
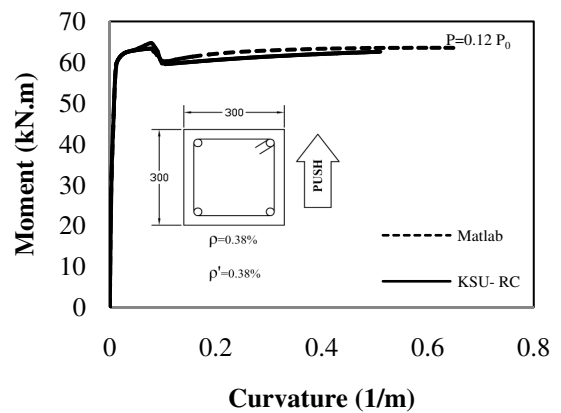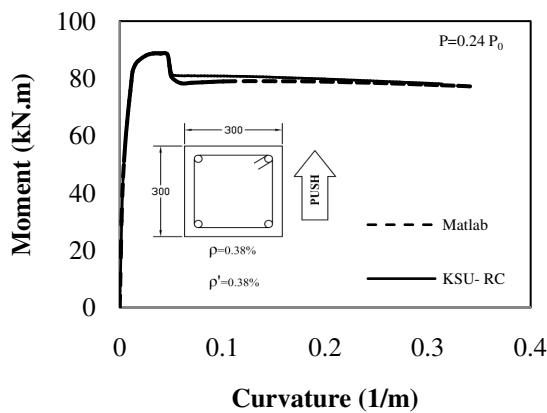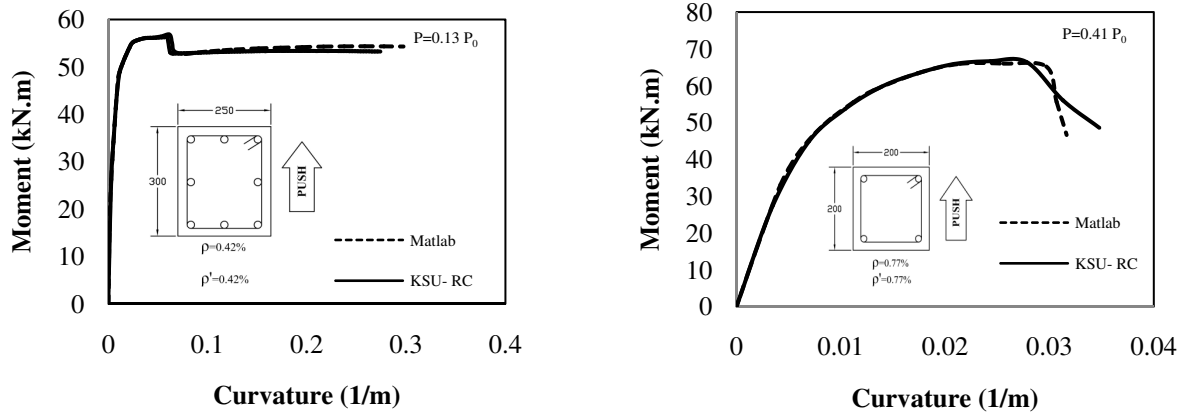
Figure 2.4. Flexural model verification

From which the current purpose is to evaluate the tension bar slip, (as shown in Fig. 2.5) the next related calculations are represented. At the first step, the elongation of bar both in column and foundation is considered.

a   **b**   **c**   **d**
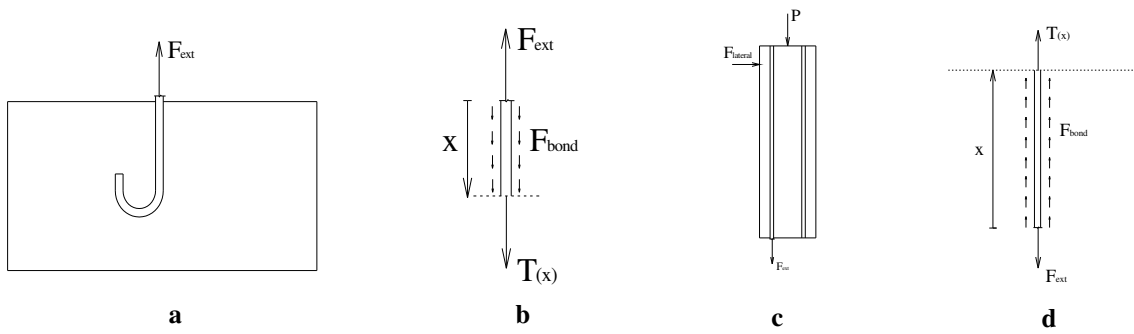
Figure 2.5. Tension bar in foundation (a) and column (c) and Free body diagram of bar in them (b and d)

$$F_{bond}(x) = \int_0^{L_{bar}} u(x)\,p\,dx \tag{2.11}$$

$$T(x) = F_{ext} - F_{bond}(x) = F_{ext} - \int_0^{L_{bar}} u(x)\,p\,dx \tag{2.12}$$

where F_{bond} is the bond resistant force, $u(x)$ is the bond distribution along the length of the bar, $T(x)$ is the internal axial force, F_{ext} is external tension force, p is the tension bar perimeter and L_{bar} is length of the bar in element (footing or column).

By assuming the steel material behavior as bilinear curve having elastic stiffness (E_1) and plastic stiffness (E_2), slippage due to tension bar elongation whether in column element or in foundation is calculated as below:

Before bar yielding: $S_{relative} = \displaystyle\int_0^{L_{bar}} \frac{T(x)}{E_1 A_S} dx$ (2.13- a)

After bar yielding: $S_{relative} = \displaystyle\int_0^{L_{bar,plastic}} \frac{T(x)}{E_2 A_S} dx + \int_{L_{bar,plastic}}^{L_{bar}} \frac{T(x)}{E_1 A_S} dx$ (2.13- b)

where $L_{bar,plastic}$ is the plastic length of the tension bar and A_S is the area of a tension bar. So in order to solving possibility for above integration, it is necessary to divide linear phase between u_A and u_W in Fig. 1.1 (a), by some uniform steps. In present model, the $[0,S_t]$ interval is divided by 100 equal steps. S_t that is known as the calibration parameter in this model varies between 1.8 mm and 3.2 mm (S_f in Fig. 1.1 (b)).

Another part of slip is due to unloaded bar end movement. It differs from bar elongation. For tension bar with hook at the unloaded end, slip model for 180 degree hook, was represented by Fabbrocino et al. (2005):

$$S_{anchor} = 3.9(f_{s,hook} / f_u)^{3.3} \tag{2.14}$$

where S_{anchor} is slip in the hook in mm, $f_{s,hook}$ is bar stress in the beginning point of hook turning (end of development length) in MPa, and f_u is the ultimate strength of bar in MPa.

$$f_{s,hook} = \frac{F_{ext} - \int_0^{L_{bar}} u(x)\,p\,dx}{A_S} \tag{2.15}$$

Fig. 2.6 shows the behavior of hook (in the footing), for an experimental specimen (SP1, Table 2.1) by using above model (p and A_s are perimeter and cross section area of hooked bar, respectively).
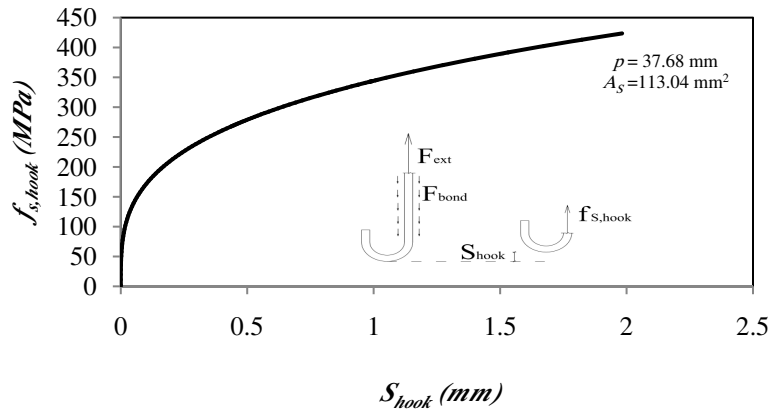

Figure 2.6. Hook behavior in footing

The bar end in column element in some experimental specimens that were used to model verification, had hook, but in others which didn't have, the slip behavior resembles those reinforced by hook at the unloaded end of the bar (at the top of column). As Arabpanahan et al. asserted, that is the result of extreme confining and pre- stressing of element at the adjacent of exerting point of lateral load. Further, slip- stress curve for bar in footing (hooked bar) and in column (confined bar) are depicted (Fig. 2.7).

By flexural solving of critical section (footing and column interface), tension stress of bar (f_{ext}) is achieved and by referring to above curves, bar total slippage in both column and footing (respectively $S_{element}$ and $S_{footing}$) can be reached. Total slip of bar at the interface of column and footing (S_{total}) is the summation of slips in element and column.

$$S_{total} = S_{element} + S_{footing} \tag{2.16}$$

where $S_{element}$ and $S_{footing}$ are slip of tension bar in column and footing, respectively.

a   **b**
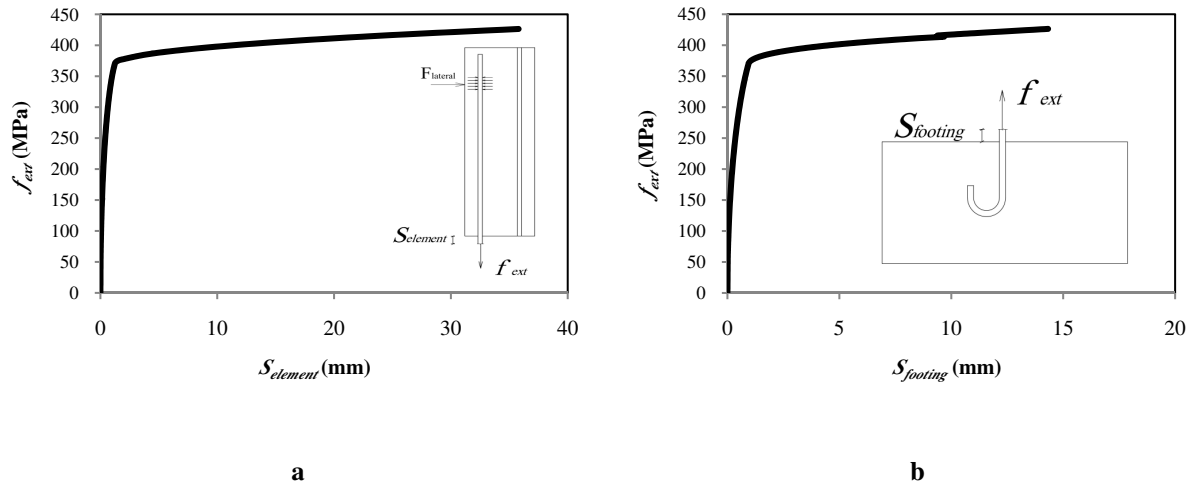
Figure 2.7. Slip behavior in element (a) and footing (b)

Finally, as Sezen and Setzler (2008) represented, the deflection at the column index point originated from slip is calculated:

$$\Delta_S = \frac{S_{total}}{d-c} L_{shear} \tag{2.17}$$

where $(d-c)$ is the uplifting depth of rocking element from base. Fig. 2.8 shows the results of numerical model compared with experimental models for same column specimens as the Base shear versus Displacement curves. Also the specifications of subjected specimens are summarized in Table 2.1 and 2.2.

**Table 2.1.** Specimens' material specifications

Specimen	Concrete	Longitudinal bars					Transverse bars		
	f'_c (MPa)	f_y (MPa)	f_u (MPa)	Φ (mm)	εy	εu	f_y (MPa)	Φ (mm)	S (mm)
SP1	23.9	370	520	4Φ12	0.0018	0.18	290	8	200
SP2	23.9	370	520	8Φ14	0.0018	0.18	290	8	200
SP3	25	355	470	6Φ12	0.0017	0.27	430	8	100
SP4	25	355	470	6Φ12	0.0017	0.27	430	8	100

Table 2.2. Geometrical and mechanical Specifications of specimens

Specimen	Shear Length (mm)	Total length (mm)	Cross section (mm^2)	$A_S = A'_S$ (mm^2)	Axial load (kN)	Normalized axial load
SP1	750	1000	250×250	226.08	225	0.15f'c Ag
SP2	750	1000	250×250	615.75	450	0.30f'c Ag
SP3	1570	2000	300×300	339	270	0.12f'c Ag
SP4	1570	2000	300×300	339	540	0.24f'c Ag

SP1, SP2, SP3 and SP4 are the same that were named WOS-C, WOC2-C (adopted from Arani's test), C270B1 and C540B1 (adopted from Verderame's test), respectively. Also A_g is the gross section of each specimen and A_S and A'_S are the area of positive and negative bars in the critical section, respectively.

Numerical model predicts backbone curve for each input specimen. For SP1 and SP2, the proposed model and also the cyclic response of column under lateral and axial load are illustrated .Experimental results for SP3 and SP4 show the backbone curve extracted from the cyclic response of these columns.
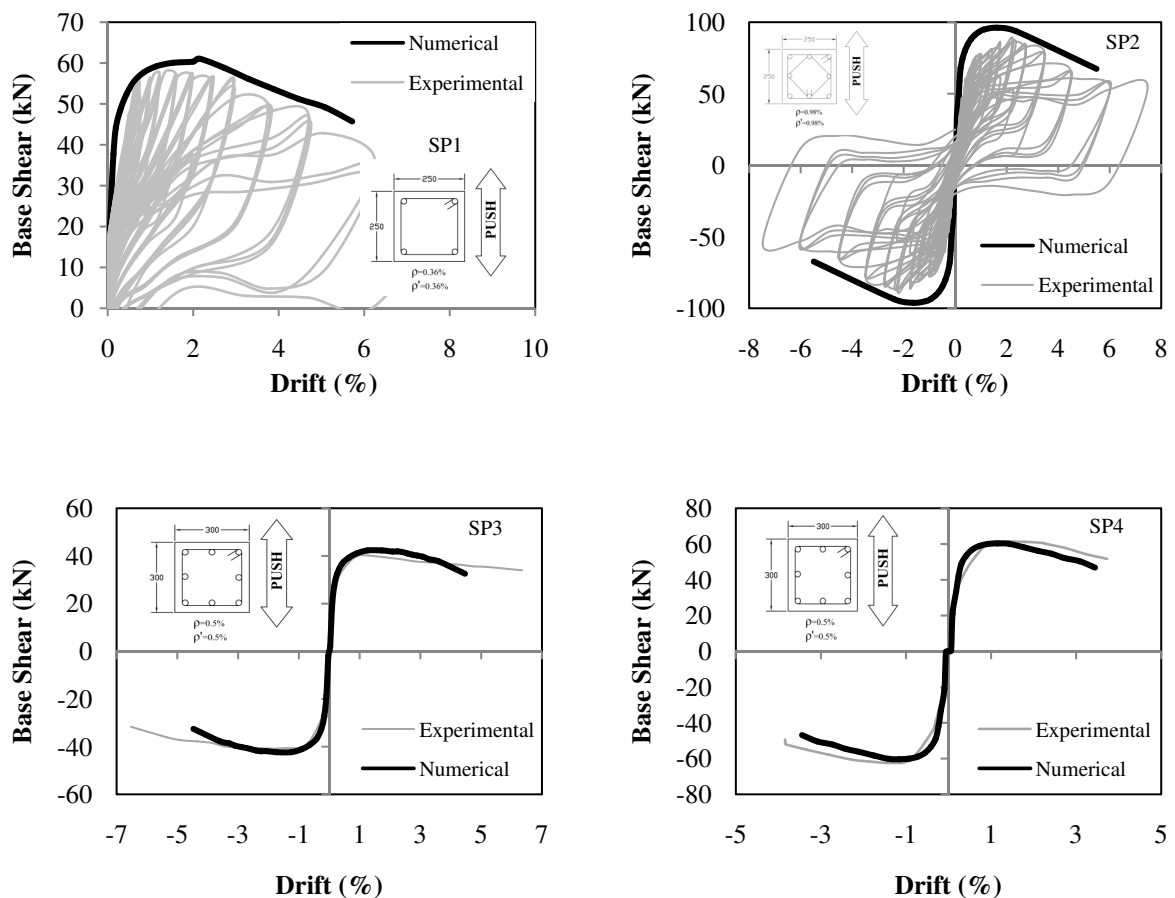
Figure 2.8. Comparison of numerical model and experimental model in total behavior

The only difference between SP3 and SP4 is the level of axial load. As it is obvious, numerical model predicts initial stiffness and strength for each of four specimens with a good approximation. Also numerical model predicts the ultimate displacement approximately near to the ultimate displacement in the experimental one, in both SP2 and SP4, but in SP1 and SP3 the experimental ultimate displacement owns the value more than numerical ones. It can be interpreted in the way that the extreme compression web in the section sustains strains more than the amount introduced in the numerical algorithm in MATLAB programming.

3. PARAMETRIC INVESTIGATION

It seems that determining of the maximum horizontal displacement is significant in the structures that are designed or assessed against seismic action, especially in those reinforced by smooth bars. In other words, because of fixed end rotation contributing in ultimate displacement or ultimate rotation, calculating of this limit can be worthwhile. In order to achieve to this aim, recognizing of parameters applied in numerical modeling and influenced on total chord rotation is necessary. These parameters consist of those that have importance in surveying of flexural and slippage displacements and also strength and initial stiffness of the element. So these parameters are known by performing trial and error steps and have been introduced in Table 3.1.

So, by having these important parameters, 20 numerical specimens were designated and made by verified model. In these specimens, it is regarded that regular varying is available for each variable (parameter). By committing a nonlinear regression analysis the next formula is achieved.

Table 3.1. Introduction of effective parameters in ultimate chord rotation

Effective Parameter	Description
f_y/f_c'	Ratio of bar yielding strength and concrete compression strength
ρ'/ρ	Ratio of negative proportional bars and positive proportional bars
L_d	Length of tension bar in footing (development length)
L_{shear}	Shear length of column
v	Ratio of exerting axial load and axial strength of column section
H/B	Section dimension ratio

Therefore the relationship in order to calculating the chord rotation is represented:

$$\theta_{CR,U} = 0.948 \left(\frac{\rho'}{\rho}\right)^{0.16} \left(\frac{f_y}{f_C'}\right)^{0.59} (L_d)^{-0.79} (L_{shear})^{-0.02} v^{-0.48} \left(\frac{H}{B}\right)^{0.76} \tag{3.1}$$

where $\theta_{CR,U}$ is ultimate chord rotation that can be seen in Fig. 4.1. Approximation of coefficients and unknown parameters was performed based on R- squared method (for this analysis, $R^2 = 0.909$). f_y and f_C' are in MPa and L_d and L_{shear} are in mm.

4. CONCLUSION

In concrete columns reinforced by smooth bars, an important behavioral characteristic is the role of rocking mode. Rocking provides significant contribution to lateral displacement of such members. The main components of displacement include: flexure, slip (fixed end rotation) and shear. The first is modelled based on a lumped plastic hinge near the footing, the second has used a bond- slip rule derived from pull-out tests. The third component involves shear deformation that is known to have low contribution in total deformation in comparison to two others. An important aspect of this paper is to clarify the concept of P-Δ that involves significant difference relative to members reinforced by ribbed bars. Also, a relationship, in order to calculate the ultimate chord rotation in this kind of columns was proposed.

REFERENCES

Analysis for reinforced concrete members (KSU-RC), Kansas State University, http://www.ce.ksu.edu/faculty/esmaeily/KSU_RC.htm

Arabpanahan, M., Marefat, M.S. and Khanmohammadi, M. (2012). Numerical simulation of flexural behaviour of concrete columns reinforced by plain bars. *4th International Conference on Seismic Retrofitting, ICSR 2012,* Tabriz, Iran, 2-4 May 2012, (submitted).

Arani, K. K., Marefat, M. S., Biucky, A. A. and Khanmohammadi, M. (2010). Experimental seismic evaluation of old concrete columns reinforced by plain bars, *Journal of the Structural Design of Tall and Special buildings*, **DOI**: 10.1002/tal.686

Fabbrocino, G., Verderame, G., Manfredi, G. and Cosenza, E. (2004). Structural models of critical regions in old-type R.C. frames with smooth rebars, *Journal of Engineering Structures* **26:6**, 2137-2148.

Feldman, L. and Bartlett, F. (2007). Bond stresses along plain steel reinforcing bars in pullout specimens, *ACI Structural Journal* **104:6**, 685-692.

Paulay, T. and Priestley, M. N. J. (1992). *Seismic Design of Reinforced Concrete and Masonry Buildings*, John Wiley & Sons, Inc., New York

Roh H, Renhorn AM.(2009). Analytical modeling of rocking elements. *Engineering Structures* **31**:**5**, 1179–1189.

Sezen, H. and Setzler, E.J. (2008). Reinforcement slip in reinforced concrete columns. *ACI Structural Journal* **105:3**, 280- 289

Verderame, G., Fabbrocino, G. and Manfredi, G. (2008a). Seismic response of R.C. columns with smooth reinforcement. Part I: monotonic tests, *Engineering Structures* **30:9**, 2277–2288.

Verderame GM, Fabbrocino G, Manfredi G. (2008b). Seismic response of R.C. columns with smooth reinforcement. Part II: cyclic tests. *Engineering Structures* **30:9**, 2289–2300.

Verderame, G., De Carlo, G., Ricci, P. and Fabbrocino, G. (2009(b)) Cyclic bond behaviour of plain bars. Part II: analytical investigation, *Construction and building Materials* **23:12**, 3512-3522.

Yalcin C, Kaya O, Sinangil M. 2008. Seismic retrofitting of R/C columns having plain bars using CFRP sheets for improved strength and ductility. *Construction and Building Materials* **22:3**, 295–307